

Avalanche breakdown characteristics of $\text{Al}_{1-x}\text{Ga}_x\text{As}_{0.56}\text{Sb}_{0.44}$ quaternary alloys

X. Zhou, S. Zhang, J. P. R. David, *Fellow, IEEE*, J. S. Ng, *Member, IEEE* and C. H. Tan, *Member, IEEE*

Abstract—Avalanche breakdown characteristics are essential for designing avalanche photodiodes. In this work, we investigated the effects of adding Ga to $\text{Al}_{1-x}\text{Ga}_x\text{As}_{0.56}\text{Sb}_{0.44}$ quaternary alloys. Using p-i-n diodes with a 100 nm i-region and alloy composition ranging from $x = 0$ to 0.15, we found that the bandgap energy of $\text{Al}_{1-x}\text{Ga}_x\text{As}_{0.56}\text{Sb}_{0.44}$ reduces from 1.64 to 1.56 eV. The corresponding avalanche breakdown voltage decreases from 13.02 to 12.05 V, giving a reduction of 64.7 mV for every percent addition of Ga. The surface leakage current was also found to be significantly lower in the diodes with $x = 0.10$ and 0.15 suggesting that Ga can be added to reduce the surface leakage current while still preserving the lattice match to InP substrate. The data from this work can be downloaded freely [1].

Index Terms—Avalanche photodiodes, AlGaAsSb, Bandgap, breakdown voltage

I. INTRODUCTION

AVALANCHE photodiodes (APDs) are widely used in optical communication system, imaging and sensing applications because their mean avalanche gain factor, M , enable them to provide higher overall sensitivity than that from conventional PIN photodiodes. As reverse bias, V , approaches avalanche breakdown voltage, V_{bd} , the APD's gain approaches infinity.

The avalanche gain is the end product of successive impact ionization events, in which an ionizing carrier gives up part of its energy to create a pair of free electron and hole. At high avalanche gains, however, the APD's bandwidth decreases with gain and its avalanche noise (characterized by excess noise factors, F) increases with gain. These characteristics ultimately determine the useful operating conditions of an APD. When designing APDs, the minimum amount of information required therefore includes V_{bd} , $M(V)$, $F(M)$ and

the limit imposed by tunnelling current. The first three pieces of information are usually obtained experimentally from appropriate test structures, because accurate simulations for these demand accurate impact ionization coefficients and threshold energies, which themselves have to be deduced from experimental V_{bd} , $M(V)$, and $F(M)$.

$\text{AlAs}_{0.56}\text{Sb}_{0.44}$ (lattice-matched to InP substrates) is a wide bandgap semiconductor material being investigated as an avalanche material for 1310 and 1550 nm wavelength APDs. It offers very small temperature coefficients (i.e. good thermal stability) [2] and very low $F(M)$ characteristics [3]. Since high composition of Al is known to be vulnerable to oxidization, which could lead to problems in reliable device fabrication, it is worthwhile to study avalanche characteristics of its related quaternary material, $\text{Al}_{1-x}\text{Ga}_x\text{As}_{0.56}\text{Sb}_{0.44}$, which is likely to have less surface oxidation [4].

In this work, we carried out experiments to accurately determine avalanche breakdown characteristics of $\text{Al}_{1-x}\text{Ga}_x\text{As}_{0.56}\text{Sb}_{0.44}$ for $x = 0$ to 0.15. The test structures were p-i-n diodes with thin avalanche layers to maximize usefulness of the results, given the emphasis on high bandwidth APDs which generally require thin, rather than thick avalanche layers. In addition, due to a lack of experimental reports, this work included experimental confirmation of minimum bandgaps, E_g , of $\text{Al}_{1-x}\text{Ga}_x\text{As}_{0.56}\text{Sb}_{0.44}$.

II. EXPERIMENTAL DETAILS

Four $\text{Al}_{1-x}\text{Ga}_x\text{As}_{0.56}\text{Sb}_{0.44}$ (hereafter referred to as $\text{Al}_{1-x}\text{Ga}_x\text{AsSb}$) homo-junction p-i-n diodes, with $x = 0, 0.05, 0.10, 0.15$, were grown on InP substrates by molecular beam epitaxy. Each of the four wafers consists of a nominal $w = 100$ nm $\text{Al}_{1-x}\text{Ga}_x\text{AsSb}$ i-layer, sandwiched by a 300 nm p^+ $\text{Al}_{1-x}\text{Ga}_x\text{AsSb}$ cladding layer (Be doping density of $2 \times 10^{18} \text{ cm}^{-3}$) and a 100 nm n^+ $\text{Al}_{1-x}\text{Ga}_x\text{AsSb}$ cladding layer (Te doping density of $2 \times 10^{18} \text{ cm}^{-3}$). The epilayers were capped with a 100 nm p^+ InGaAs and a 1000 nm n^+ InGaAs contact layers for good ohmic contact. Lattice matching of the $\text{Al}_{1-x}\text{Ga}_x\text{AsSb}$ epilayers to InP was confirmed by post growth high resolution X-ray diffraction (XRD) measurements. Estimated Sb composition were 42.8, 46.7, 44.4 and 44.1 % for the $x = 0, 0.05, 0.10, 0.15$ wafers, respectively. The largest lattice mismatch ($x = 0.05$ wafer) was < 0.24 %.

Manuscript submitted June, 2016. This work was supported by the UK Engineering and Physical Sciences Research Council (EPSRC) (grants EP/K001469/1), the Royal Society (University Research Fellowship for J. S. Ng) and the EU Marie-Curie Training Network PROMIS (grant H2020-MSCA-ITN-2014-641899).

X. Zhou, S. Zhang, J. P. R. David, J. S. Ng and C. H. Tan are with the Department of Electronic and Electrical Engineering, The University of Sheffield, George Porter Building, Wheeldon Street, Sheffield S3 7HQ, U.K. (e-mail: x.zhou@sheffield.ac.uk; shiyong.zhang@sheffield.ac.uk; j.p.david@sheffield.ac.uk; j.s.ng@sheffield.ac.uk and c.h.tan@shef.ac.uk).

Copyright (c) 2016 IEEE.

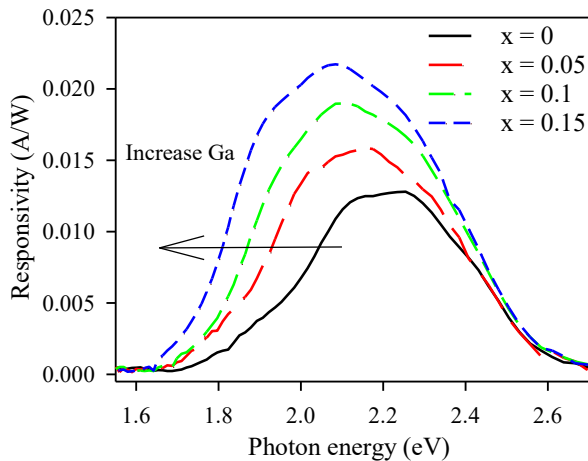


Fig. 1. Zero bias responsivity versus photon energy from diodes of the four wafers.

TABLE I
BANDGAP OF $Al_{1-x}Ga_xAsSb$ ($x = 0$ TO 0.15)

x	E_g (eV)		
	interpolation	E_g^X fitting	E_g^I fitting
0	1.65	1.64	1.95
0.05	1.63	1.61	1.87
0.10	1.61	1.59	1.82
0.15	1.59	1.56	1.77

The wafers were fabricated into circular mesa diodes with diameters, D , of 400, 200, 100 and 50 μm by standard photolithography and wet chemical etch. Ti-Au was used for both p and n metal contacts. Surface passivation was not performed in this work.

All measurements on the fabricated mesa diodes were performed at room temperature, unless otherwise stated. For a given type of measurement and a given wafer, several diodes were measured. Characterization began with current-voltage (I - V) and capacitance-voltage (C - V) measurements.

Avalanche gain as a function of reverse bias measurement was performed, using a continuous-wave 543 nm wavelength HeNe laser to produce photocurrent flowing through the diode-under-test. Phase-sensitive detection of the photocurrent (chopped laser beam and lock-in amplifier) was employed to minimize the influence of dark current and background noise on the photocurrent. The laser wavelength was chosen to ensure sufficient photocurrent. Care was taken to ensure light is injected in the optical window to avoid photogenerated carriers at the sidewall. Detailed knowledge of the laser light absorption profiles, essential for experimental work deducing ionization coefficients, are not necessary for this work. To yield M , the photocurrent was normalized to primary photocurrent estimated by extrapolating from the photocurrent at low reverse bias [5]. Extrapolating the inverse avalanche gains to zero (i.e infinitely large M) gave values of V_{bd} .

Experimental confirmation of bandgaps of the $Al_{1-x}Ga_xAs_{0.56}Sb_{0.44}$ compositions used in this work relied on spectral response measurements of the diodes. These were obtained using a 100 W tungsten halogen lamp, a monochromator, and a diffraction grating with 400 nm blaze wavelength. The system response of the spectral response setup was calibrated using a commercial Si photodiode

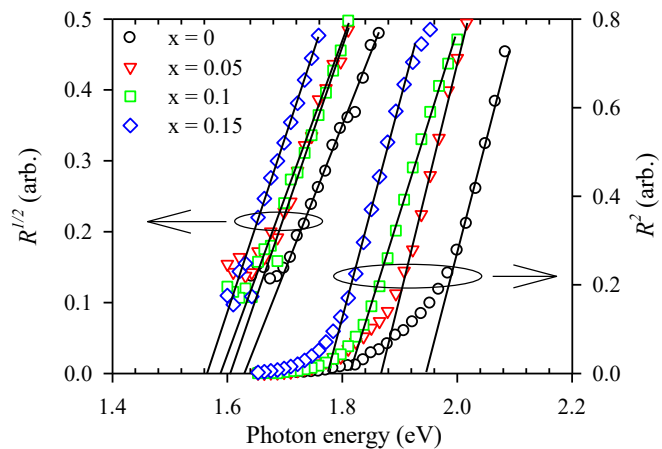


Fig. 2. Experimental results (symbols) of root (left) and square (right) of responsivity of $Al_{1-x}Ga_xAsSb$ diodes at zero external bias. The fittings (lines) are used to estimate the indirect (left) and direct energy gaps (right).

(S5973-02).

III. BANDGAP

There is no relevant experimental report on minimum bandgaps of $Al_{1-x}Ga_xAs_{0.56}Sb_{0.44}$. Since $AlAs_{0.56}Sb_{0.44}$ is an indirect bandgap material [6], the minimum bandgap of 1.65 eV observed in quantum efficiency data of [7] is its X valley bandgap, E_g^X . Using E_g^X values of 1.65 and 1.23 eV for $AlAs_{0.56}Sb_{0.44}$ and $GaAs_{0.56}Sb_{0.44}$ valley [6], respectively, linear interpolation was carried out to estimate E_g^X values for our samples, which are summarized in Table I.

Analyses of our responsivity versus photon energy, $R(\hbar\omega)$, data obtained from the diodes at 0 V, shown in Fig. 1, allowed us to assess accuracy of the values from interpolation. The responsivity values are generally low due to the attenuating effect of the top InGaAs contact layer. In our structures, the 100 nm thick InGaAs layer absorbs a significant portion of the incident light in the wavelength range measured. However the photogenerated carriers in the InGaAs layer will not contribute significant photocurrent due to the large bandgap mismatch to AlGaAsSb. Consequently the measured responsivity values are low and do not represent the actual responsivity value that can be obtained from the AlGaAsSb diodes. As Ga composition increases, the responsivity curve shifts to smaller photon energy, corresponding to narrower bandgaps. When $(\hbar\omega - E_g) \rightarrow 0$, $R \propto \alpha$, where α is the absorption coefficient, because drift current becomes dominant in the total photocurrent measured. From ref. [8, 9], the absorption coefficients for direct and indirect bandgap materials are

$$\alpha^{direct}(\hbar\omega) \propto (\hbar\omega - E_g)^{1/2}$$

and

$$\alpha^{indirect}(\hbar\omega) \propto (\hbar\omega - E_g \pm \hbar\Omega)^2,$$

respectively, where $\pm\hbar\Omega$ is the phonon energy. Linear extrapolations of R^2 (for E_g^I) and $R^{1/2}$ (for E_g^X) over different portions of the data to the photon energy axis are shown in Fig. 2 and the E_g values obtained are shown in Table I. With less than 2 % difference between our E_g^X and the interpolation values (possibly caused by slight variation in the Sb

TABLE II
C-V FITTING PARAMETER FOR $Al_{1-x}Ga_xAsSb$ DIODES

x	ϵ_r	V_{bi} (V)	Cladding doping p=n ($\times 10^{15} \text{ cm}^{-3}$)	i-region doping ($\times 10^{16} \text{ cm}^{-3}$)	w (nm)
0	10.93	1-2	1.9	2	111-105
0.05	11.09	1-2	1.8	2	116-110
0.1	11.25	1-2	1.85	2	114-108
0.15	11.41	1-2	1.75	2	110-104

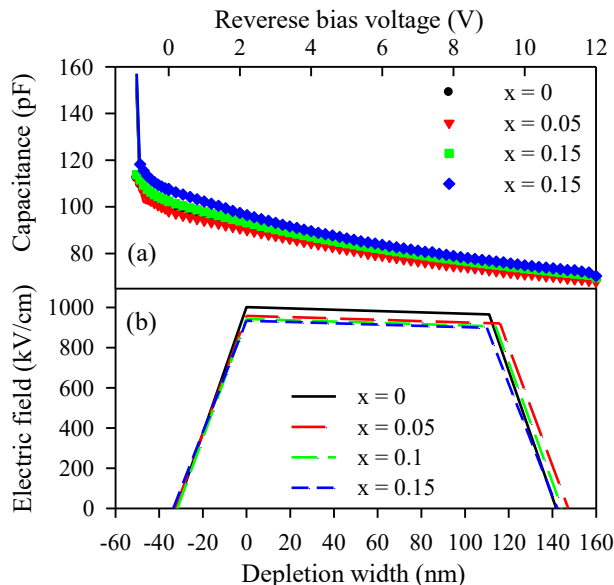


Fig. 3. (a) Measured (symbols) and fitted (lines) capacitance-voltage results for $Al_{1-x}Ga_xAsSb$ diode with $D = 400 \mu\text{m}$ at room temperature; (b) Electric field profiles of the diodes at breakdown voltages.

composition and excluding the phonon energy), there is now a set of E_g values available for analyses in the main work of V_{bd} .

IV. AVALANCHE BREAKDOWN VOLTAGE

Fig. 3(a) shows the experimental $C-V$ results and fitting carried out using 3-region electrostatic model. Due to the thin avalanche layer, the diodes are fully depleted at 0 V. Extrapolation of $1/C^2$ at small forward bias suggests the built-in potential, V_{bi} , of 1 to 2 V. Assuming relative dielectric constants, ϵ_r , in Table II, the $C-V$ fitting yielded estimates on doping densities and w , which are summarized in Table II. The relative dielectric constants were deduced through interpolation between values for AlAs [10], AlSb [11] and GaAsSb [12]. Electric field profiles, assuming the upper value of w at breakdown voltage for the four wafers are compared in Fig. 3(b).

Forward and reverse dark $I-V$ data cover diodes with four different diameters, with multiple diodes for a given diameter. Analyses of the forward $I-V$ data produced series resistances of 60 to 115 Ω and ideality factors of 1.7 - 1.8 for all four layers, suggesting that the measured forward currents are dominated by recombination currents.

For reverse dark $I-V$ data, for a given diode's junction area, the measured dark current reduces as Ga composition increases. Analyses of dark current densities from different-sized diodes (not shown here) indicate that, for all wafers, the measured dark currents contained significant surface leakage

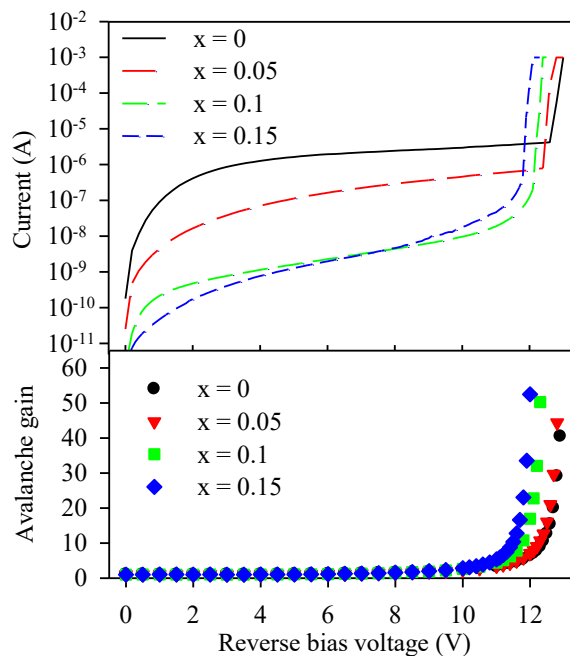


Fig. 4. Measured dark $I-V$ characteristic (top), and avalanche gain from phase-sensitive photocurrent measurements (bottom) for $Al_{1-x}Ga_xAsSb$ diodes with $D = 400 \mu\text{m}$ at room temperature.

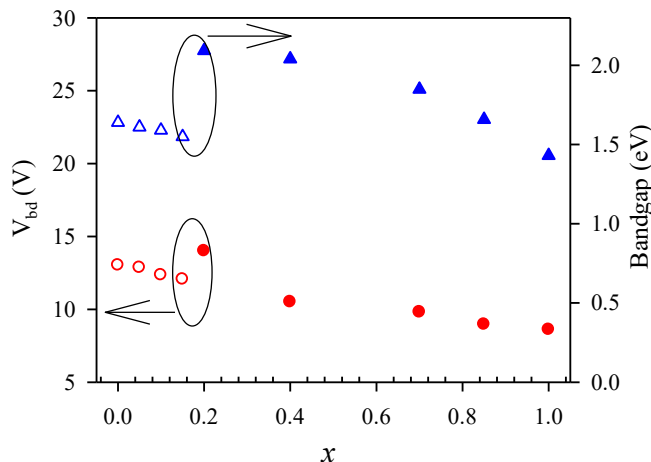


Fig. 5. V_{bd} (left axis) and energy band gap (right axis) for $Al_{1-x}Ga_xAsSb$ (open symbols) and $Al_{1-x}Ga_xAs$ (closed symbols) [13-16].

current, because the data do not scale with device area. For clarity, only the dark currents of $400 \mu\text{m}$ devices from all four samples are shown in Fig. 4. Assuming dark current breakdown condition as reverse dark current of 1 mA, the dark current's V_{bd} reduces with increasing Ga composition. It is unlikely that the values of V_{bd} obtained from dark current data are affected by series resistances in these diodes (which are not excessive), but edge breakdown (at the mesa surface) remains a possibility. More accurate values of V_{bd} were obtained from avalanche gain data, which are shown in Fig. 4. Breakdown voltages deduced from the dark current and avalanche gain are in agreement, suggesting an absence of edge breakdown on these devices.

The values of V_{bd} obtained from avalanche gain data are plotted in Fig. 5. V_{bd} decreases from 13.02 to 12.05 V, as x increases from 0 to 0.15, producing a reduction of 64.7 mV for every percent of Ga added. These are compared to

experimental values of V_{bd} from $\text{Al}_{1-x}\text{Ga}_x\text{As}$ p-i-n diodes with nominal $w = 100$ nm [13, 14], also shown in Fig. 5. Bandgap values for $\text{Al}_{1-x}\text{Ga}_x\text{AsSb}$ (Section III) and $\text{Al}_{1-x}\text{Ga}_x\text{As}$ [15, 16] are plotted in the right axis of the same figure. Both materials exhibit decreasing V_{bd} with increasing x , which corresponds to decreasing bandgap. This is not surprising because, in general, smaller bandgap materials have higher ionization coefficients for a given electric field. Hence for a given avalanche layer thickness, a smaller voltage and hence electric field is required to reach avalanche breakdown.

V. CONCLUSION

Four $\text{Al}_{1-x}\text{Ga}_x\text{As}_{0.56}\text{Sb}_{0.44}$ p-i-n diode wafers with Ga composition of $x = 0, 0.05, 0.1, 0.15$ were grown and characterized. Values of V_{bd} for the p-i-n diodes were determined and they decrease with increasing Ga composition, due to decreasing energy band gap. The band gap (direct and indirect) values were estimated from experimental photoresponse results. In addition, the p-i-n diodes' dark current characteristics exhibited a strong dependence with Ga composition, with lower surface leakage current for diodes with higher Ga content.

ACKNOWLEDGMENT

The authors would like to thank Mr Manuel Moreno Guerrero (formerly at The University of Sheffield) for preliminary work.

REFERENCES

[1] <https://dx.doi.org/10.15131/shef.data.3479396>

- [2] S. Xie and C. H. Tan, "AlAsSb avalanche photodiodes with a sub-mV/K temperature coefficient of breakdown voltage," *IEEE J. Quantum Electron.*, vol. 47, no. 11, pp. 1391-1395, Nov. 2011.
- [3] J. Xie, S. Xie, R. C. Tozer, and C. H. Tan, "Excess noise characteristics of thin AlAsSb APDs," *IEEE Trans. Electron Devices*, vol. 59, no. 5, pp. 1475-1479, May 2012.
- [4] S. K. Mathis, K. H. A. Lau, A. M. Andrews and E. M. Hall, "Lateral oxidation kinetics of AlAsSb and related alloys lattice matched to InP," *J. Appl. Phys.*, vol. 89, no. 4, pp. 2458-2464, Feb. 2001.
- [5] M. H. Woods, W. C. Johnson, and M. A. Lampert, "Use of a schottky barrier to measure impact ionization coefficients in semiconductors," *Solid-St. Electron.*, vol. 16, no. 3, pp. 381-394, Mar. 1973.
- [6] S. Adachi, *Properties of semiconductor alloys: group-IV, III-V and II-VI semiconductors*. Sussex, U.K.: Wiley, 2009, pp. 133-228.
- [7] R. E. Welsler, A. K. Sood, R. B. Laghumavarapu, D. L. Huffaker, D. M. Wilt, N. K. Dhar, and K. A. Sablon, "The Physics of High-Efficiency Thin-Film III-V Solar Cells," in *Solar Cells - New Approaches and Reviews*, L. A. Kosyachenko, Ed. USA: InTech, Oct. 2015, pp. 247-277.
- [8] L. H. Hall, J. Bardeen and F. J. Blatt, "Infrared absorption spectrum of germanium," *Phys. Rev.*, vol. 95, no. 2, pp. 559-560, Jul. 1954.
- [9] M. Fox, *Interband absorption in Optical Properties of Solids*, Oxford, U.K.: Oxford University Press, 2001, pp. 49-75.
- [10] R. E. Fern and A. Onton, "Refractive index of AlAs," *J. Appl. Phys.*, vol. 42, no. 9, pp. 3499-3500, Aug. 1971.
- [11] A. De and C. E. Pryor, "Optical dielectric functions of wurtzite III-V semiconductors," *Phys. Rev. B*, vol. 85, pp. 125201, 2012.
- [12] M. E. Levinshtein, S. L. Rumyantsev, M. Shur, *Handbook Series on Semiconductor Parameters: Vol. 2*. World Scientific: Nov. 1996.
- [13] S. A. Plimmer, J. P. R. David, G. J. Rees, R. Grey, D. C. Herbert, D. R. Wright, and A. W. Higgs, "Impact ionization in thin $\text{Al}_x\text{Ga}_{1-x}\text{As}$ ($x = 0.15-0.30$) p-i-n diodes," *J. Appl. Phys.*, vol. 82, no. 3, pp. 1231-1235, Aug. 1997.
- [14] B. K. Ng, J. P. R. David, S. A. Plimmer, G. J. Rees, R. C. Tozer, M. Hopkinson and G. Hill, "Avalanche multiplication characteristics of $\text{Al}_{0.8}\text{Ga}_{0.2}\text{As}$ diodes," *IEEE Trans. Electron Devices*, vol. 48, no. 10, pp. 2198-2204, Oct. 2001.
- [15] D. E. Aspnes, S. M. Kelso, R. A. Logan and R. Bhat, "Optical properties of $\text{Al}_x\text{Ga}_{1-x}\text{As}$," *J. Appl. Phys.*, vol. 60, no. 2, pp. 754-767, Jul. 1986.
- [16] H. J. Lee, L. Y. Juravel, J. C. Woolley and A. J. SpringThorpe, "Electron transport and band structure of GaAlAs alloys," *Phys. Rev. B*, vol. 21, no. 2, pp. 659-669, Jan. 1980.